Nanoscale Res Lett (2010) 5:597–602
DOI 10.1007/s11671-009-9512-6

NANO EXPRESS

Well-aligned Nickel Nanochains Synthesized by a Template-free Route

Pengwei Li · Rongming Wang · Weimeng Chen · Chinping Chen · Xingyu Gao · A. T. S. Wee

Received: 3 November 2009 / Accepted: 10 December 2009 / Published online: 25 December 2009
© The Author(s) 2009. This article is published with open access at Springerlink.com

Abstract Highly uniform and well-aligned one-dimensional Ni nanochains with controllable diameters, including 33, 78, and 120 nm, have been synthesized by applying an external magnetic field without any surface modifying agent. The formation can be explained by the interactions of magnetic dipoles in the presence of applied magnetic field. Magnetic measurements demonstrate that the shape anisotropy dominates the magnetic anisotropy. The demagnetization factor, ΔN, is in the range of 0.23–0.36.

Keywords Ni nanostructure · Magnetic anisotropy · X-ray absorption spectroscopy · Electron microscopy

Introduction

In the past few years, magnetic nanostructures have aroused considerable interests due to their exceptional properties and potential applications in catalysis, sensors, high-density magnetic records, bio-imaging, and many other domains [1–6]. Because most physical and chemical properties of these nanoparticles depend on their sizes and shapes, the shape control of nanostructures has become a new and interesting research field [7–9]. In particular, one-dimensional (1D) magnetic nanostructures have become one of the focused points [10–13].

Recently, magnetic field-assisted hydrothermal process has been proven to be an efficient way for directing the growth of 1D magnetic material [14–18]. However, previous investigations indicated that the surfactants such as polyvinyl pyrrolidone, hexadecylamine, and cetyltrimethyl ammonium bromide were still necessary, and the diameters of the fabricated nanochains were usually larger than 100 nm [15, 18–20]. Template-free magnetic field-induced synthesis of well-aligned Ni nanochains with smaller diameters has rarely been reported [14].

Hence, in this work, we proposed a magnetic field-induced solution-phase synthesis and self-assembly approach of aligned Ni nanochains using environment-friendly reagents. The growth mechanism and the magnetic anisotropy of the Ni nanochains have been discussed in terms of the applied magnetic field.

Experimental

Setup and Apparatus

Figure 1a shows a simple sketch for the setup (drawn not to scale). The magnetic poles have a diameter of 10 cm with a distance of about 8 cm in between. A magnetic field from 0 to 5 kOe is available between the poles for the experiment by supplying an electric current from 0 to 10 A to the coils. A three-necked flask wrapped with a heating tape is placed

P. Li · R. Wang (✉)
Key Laboratory of Micro-Nano Measurement-Manipulation and Physics (Ministry of Education) and Department of Physics, Beijing University of Aeronautics and Astronautics, 100191 Beijing, People's Republic of China
e-mail: rmwang@buaa.edu.cn

W. Chen · C. Chen (✉)
Department of Physics, Peking University, 100871 Beijing, People's Republic of China
e-mail: cpchen@pku.edu.cn

X. Gao · A. T. S. Wee
Departments of Physics, National University of Singapore, Singapore 117542, Republic of Singapore

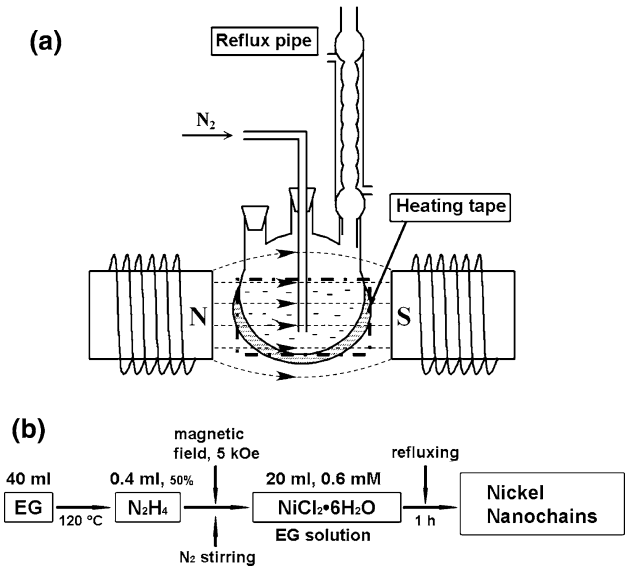

Fig. 1 **a** A simple sketch for the setup. A homogenous magnetic field from 0 to 5 kOe is available for the experiment by varying the electric current from 0 to 10 A. **b** Flowchart for a typical synthesis process

in the center between the magnetic poles for the field-induced synthesis of Ni nanochains.

Magnetic field-induced Synthesis of Nickel Nanochains

All chemicals used in this experiment were analytical grade and used without further purification. In a typical experiment, 40 ml ethylene glycol (EG) was first put into a three-necked flask and heated up to 120°C by a heating tape. Then a 0.4-ml solution of hydrated hydrazine (50%) was added and maintained at 120°C for 5 min. An external magnetic field (5 kOe) was applied, and 20-ml as-prepared $NiCl_2{\cdot}6H_2O$ solution of 6×10^{-4} mol/l (2.9 mg, dissolved in 20 ml EG, room temperature) was added into the flask. The whole solution was stirred by flowing N_2 gas of 20 ml/min at all times. After refluxing for 1 h, a black product was obtained, filtrated, and then rinsed with ethanol and deionized water for 5–6 times. The synthesis process is summarized in the flowchart in Fig. 1b.

In this report, three nickel nanochains with average diameters of 33 ± 3 (sample 1), 78 ± 8 (sample 2), and 120 ± 12 nm (sample 3) have been synthesized at temperature of 150, 120, and 90°C, respectively. More than three runs have been made for reproduction at each fixed temperature and magnetic field. The diameter of the nanochains is analyzed statistically from the images of about 100 randomly selected nanochains appeared in a scanning electron microscopy (SEM) micrograph of the sample. The standard deviation is determined as about 10%. The influence of the applied magnetic field on the morphologies of the nanochains has also been investigated.

Magnetic field-induced Reorientation of Nickel Nanochains

To obtain well-aligned Ni nanochains array, freshly synthesized nickel nanochains were each dispersed in ethanol and ultrasonically washed for 10 min. Then, the suspension was dropped onto the silicon slice under a 2-kOe magnetic field and dried in air.

Characterization Methods

The structural and chemical information of the as-prepared products was studied using X-ray diffraction (XRD, X'Pert Pro MPD system, Cu K_α), scanning electron microscopy (SEM, S-4800, Hitachi Company), transmission electron microscopy (TEM, 2100F, JEOL Company) equipped with an energy dispersive X-ray spectroscopy (EDS) apparatus, and X-ray absorption spectroscopy (XAS) with sample current in total electron yield mode at SINS beamline at Singapore Synchrotron Light Source [21]. For the XRD and XAS measurements, powder samples were used. The SEM micrographs were taken with the nanochains dispersed over the silicon substrates. For the TEM, high-resolution TEM (HRTEM) observations and EDS analysis, the as-grown nanochains were dispersed in ethanol and dropped onto a carbon film supported on a copper grid and dried in air. Magnetic properties of the as-synthesized nanochains were measured using a superconducting quantum interference device (SQUID) magnetometer (Quantum Design), with the nanochains prepared over the silicon substrates.

Results and Discussions

Detailed results of characterization for sample 1 are presented as follows. Figure 2a, b shows typical morphologies of the as-prepared samples obtained without and with magnetic field of 5 kOe at 150°C, respectively. Curly interlaced net-like chain structures synthesized without magnetic field are vivid in Fig. 2a, with diameters of 35 ± 5 nm and lengths of up to 500 nm. Figure 2b shows the sample (sample 1) synthesized under an external 5-kOe magnetic field. The nanochains are axially aligned and relatively uniform in size (33 ± 3 nm in diameter, and 1–2 μm in length). The morphologies are obviously different without and with the presence of applied field, as revealed by Fig. 2a, b, attributed to the field-driven alignment effect. For the axially aligned sample shown in Fig. 2b, the random orientation of the freshly synthesized

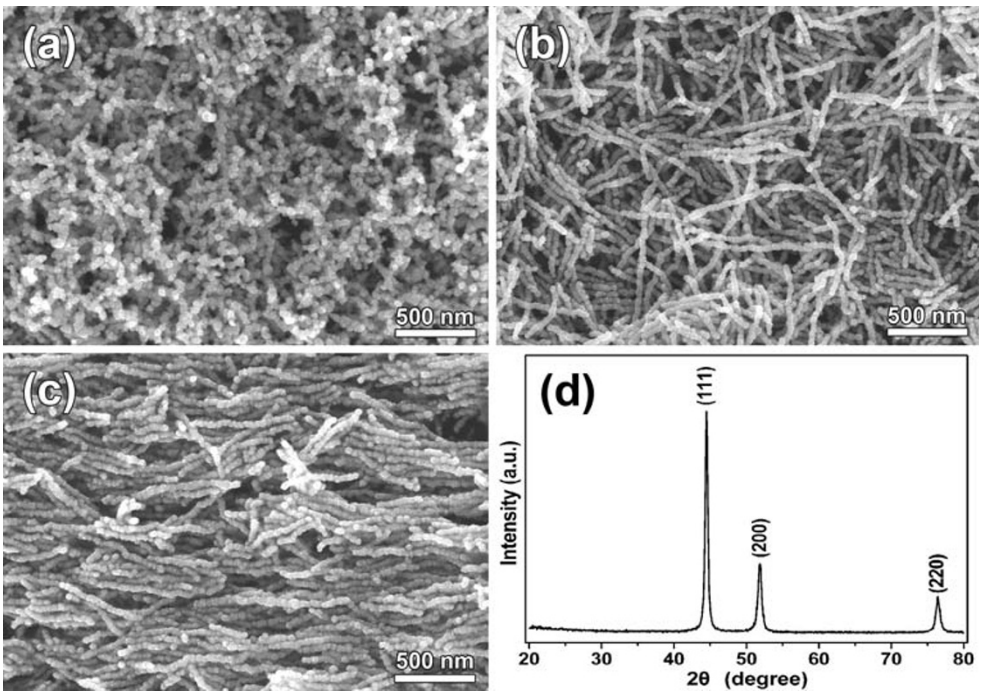

Fig. 2 Typical SEM micrographs of nickel nanochains. **a** without magnetic field showing a dendritic morphology, **b** with a magnetic field of 5 kOe applied during the synthesis process, showing an axially aligned structure, **c** reorientation of the axially aligned Ni nanochains on a silicon substrate by a 2-kOe magnetic field. **d** XRD pattern of the powder sample shown in **b**

nanochains is mainly caused by the stirring and rinsing processes in the experiment. These axially aligned Ni nanochains can be orderly reoriented by drying a droplet of sample solution, which is prepared by dispersing the nanochains in ethanol, over the silicon substrate in the presence of an applied field (20 kOe), as shown in Fig. 2c. This reveals the dipolar properties of the whole nanochain along the chain axis. For each individual nanochain, the local direction of the nanoparticles deviates from the axial direction with a small angular distribution, which is expected to be of a Gaussian type [18]. The crystal phase of all the samples was examined by using X-ray diffraction technique. A typical X-ray diffraction result of sample 1 is shown in Fig. 2d. The observed X-ray reflections can be well indexed with lattice parameters of face-centered cubic (f.c.c.) Ni (JCPDF No. 04-0850).

The chemical compositions of the as-synthesized sample were characterized by EDS. Figure 3a is for the EDS spectrum of sample 1. It reveals that the as-synthesized nanochains are metallic Ni, except that the carbon and copper peaks from the carbon film and copper grid. XAS investigation further supports the metallic nature of the sample. The spectra have been normalized at far end somewhere without subtraction of the step function [21], as shown in Fig. 3b. The $L_{2,3}$-edge XAS spectrum of the nanochains is consistent with those of pure metallic Ni foil except that the $L_{2,3}$ peak intensities in our experiment are ~30% stronger. Hence, the nanochains have more 3d holes than the metallic Ni foils, which is attributable to the small size effect [22].

To characterize the microstructure, we carried out TEM and HRTEM investigations. Figure 4a shows a typical bright-field TEM image of a single nanochain (sample 1) corresponding to the nanochains shown in Fig. 2b. The single particle and the joint part of two adjacent nanoparticles, which are marked with frames "I" and "II" in Fig. 4a, are further investigated by HRTEM and are shown in Fig. 4b, c, respectively. Lattice fringes throughout the entire HRTEM images reveal the crystalline nature of the nanoparticle. The interplanar spacing in Fig. 4b, c is measured to be 0.203 and 0.176 nm, which agree well with those between {111} and {200} planes of Ni crystal, respectively. Detailed investigations reveal that each individual nanoparticle essentially consists of several single-crystalline grains with a typical size of 10–20 nm. The observed size of the grain agrees well with the estimated value about 14 nm from the XRD data using Scherrer's equation. The selected area electron diffraction (SAED) pattern of the as-prepared nanochains (inset of Fig. 4b) confirms that the synthesized nanomaterial is metallic Ni with f.c.c. structure.

As illustrated in Fig. 5, a three-step model is proposed to explain the growth mechanism of the well-aligned Ni nanochains. In the first step, the primary Ni nanocrystallites nucleate and grow. Then, they aggregate to form nanoparticles, the size of which depends on the reaction temperature, hence is dictated mainly by the thermal agitation energy. Finally, these nanoparticles reach the size of thermal equilibrium and are self-assembled into nanochains by the alignment effect in the applied magnetic field. In this

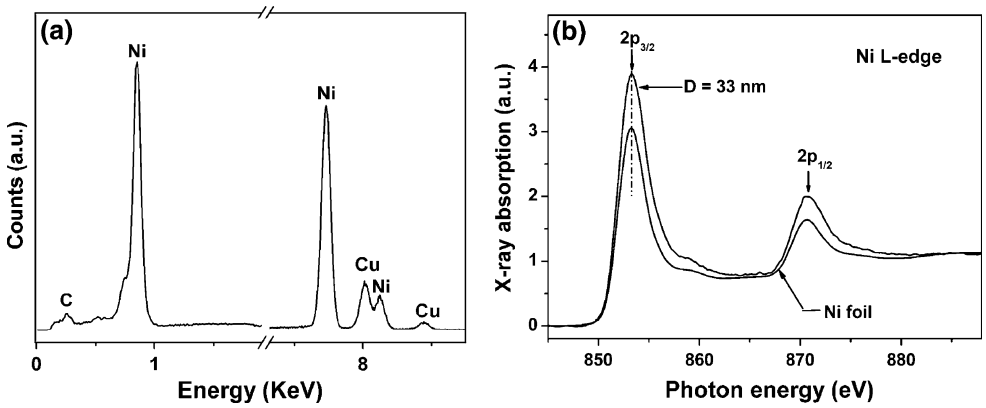

Fig. 3 **a** EDS profile and **b** L-edge XAS spectrum of the as-synthesized nickel nanochains (sample 1). The XAS spectrum has been normalized at far end somewhere without subtraction of the step function [21]

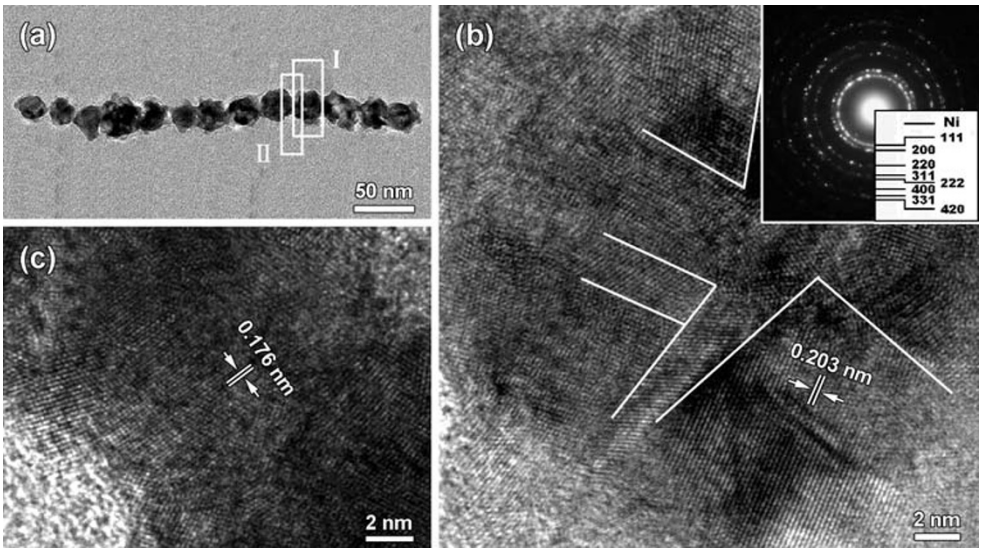

Fig. 4 **a** TEM image of an individual Ni nanochain. **b** and **c** HRTEM images of areas "I" and "II" in **a**. The inset of **b** is the corresponding SAED pattern

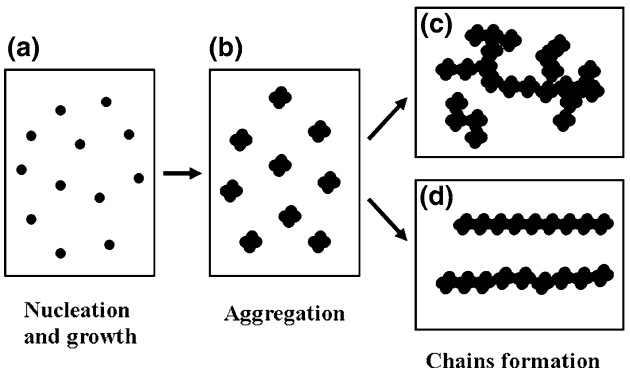

Fig. 5 Schematic diagram for the growth mechanism of the Ni nanochains. **a** Processes of nucleation and growth, **b** aggregation processes, **c** self-assembly processes for the chain formation in dendritic morphology, and **d** under applied magnetic field for the formation of axially aligned nanochains

formation process, the competition between the magnetic field energy and the thermal agitation energy of the nanoparticles plays an important role. Without the magnetic field, the dendrite structure is observed, as shown in Fig. 2a. The thermal agitation energy dominates the thermodynamic driving forces and results in a structure of random alignment [23].

The in-plane field-dependent magnetization of the samples was measured by a SQUID magnetometer, with the applied field parallel and perpendicular to the direction of the aligned nanochains on the silicon substrate. The hysteresis loops measured at 5 K are plotted in Fig. 6, for (a) sample 1 with diameter of 33 ± 3 nm, (b) sample 2 with diameter of 78 ± 5 nm, and (c) sample 3 with diameter of 120 ± 12 nm. The diamagnetic background of the Si-substrate, with the susceptibility $\chi = -1.6 \times 10^{-8}$ emu/Oe, as

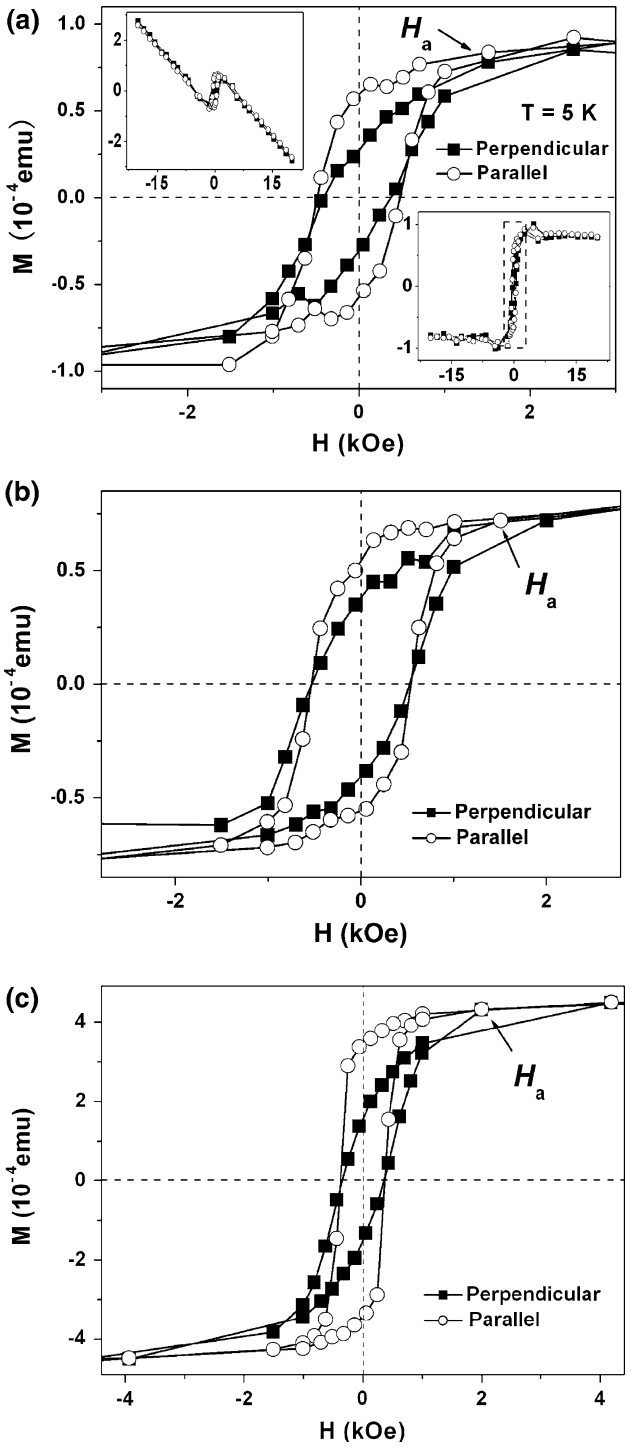

Fig. 6 In-plane field-dependent $M(H)$ curves measured at $T = 5$ K, with the applied field perpendicular (*solid square*) and parallel (*open circle*) to the axial direction of the nanochains with the sizes of **a** 33 ± 3 nm, **b** 78 ± 5 nm, and **c** 120 ± 12 nm. The *upper left inset* of **a** shows the $M(H)$ curve with the diamagnetic background of silicon substrate. The *lower right inset* shows the $M(H)$ curve by subtracting the diamagnetic contribution from the substrate

shown in the upper left inset of Fig. 6a, has been subtracted. There is obvious difference between the two hysteresis curves, i.e., the tilting of the open loops, attributed to the shape anisotropy [24, 25]. To estimate the anisotropy by the expression, $K = \mu_0 M_S H_A/2$ [26], the saturation magnetization of the bulk value of Ni, $M_S = 485$ emu/cm^3, is adopted, and the anisotropy field $H_A \sim 1.5$ kOe is determined in Fig. 6a, at which the curves of the parallel and perpendicular loops bifurcate. The anisotropy is then obtained as $K \sim 3.6 \times 10^4$ J/m^3. It is larger than the bulk value of magneto-crystalline anisotropy, $\sim 4.5 \times 10^3$ J/m^3, by one order of magnitude. Obviously, the shape anisotropy dominates the magneto-crystalline anisotropy in this case. The demagnetization factor of the shape anisotropy is determined as $\Delta N \sim 0.24$ according to the expression $K = \frac{1}{2}\,\mu_0 \Delta N\, M_S^2$. For samples 2 and 3, the anisotropy fields H_A are determined as ~ 1.5 and 2.0 kOe in Fig. 6b, c, respectively. The corresponding demagnetization factors thus obtained are $\Delta N \sim 0.24$ and 0.32. These values are slightly larger than that of 50-nm nickel nanochains in a powder collection [27], $\Delta N \sim 0.19$, and is about the same as that of nickel nanowires [28], with the size of about 12–50 nm, $\Delta N = 0.23$–0.36.

For the axially aligned nanochains dispersed over the Si-substrate as shown in Fig. 2c, an interesting feature is observed. The nanochains appear to bundle up, 5 or 6 in each bundle. This is an indication that there exists intra-chain dipolar interaction which is likely to be of anti-ferromagnetic ordering, as revealed by the work of Bliznyuk et al. [29]. This is an interesting issue to study. However, it is difficult to show evidence for this property by the magnetization measurements alone in the present work.

Conclusions

A facile and effective field-induced method has been employed to prepare highly uniform, size-controllable, well-aligned Ni nanochains without any surface active agent. The formation can be explained by the interactions of magnetic dipoles in the presence of applied magnetic field. In-plane $M(H)$ curves with the applied field parallel and perpendicular to the direction of the aligned nanochains indicate that the shape anisotropy is a significant factor for the magnetization reversal. The greatly enhanced magnetic anisotropy of the well-aligned magnetic nanochains implies their potential applications in the fields of magnetic records, magnetic switches, etc.

Acknowledgments This work was supported by the National Natural Science Foundation of China (Nos. 50671003 and 10874006), the National Basic Research Program of China (Nos. 2009CB939901 and 2010CB934601), and the Program for New Century Excellent Talents in University (NCET-06-0175).

Open Access This article is distributed under the terms of the Creative Commons Attribution Noncommercial License which permits any noncommercial use, distribution, and reproduction in any medium, provided the original author(s) and source are credited.

References

1. N.A. Frey, S. Peng, K. Cheng et al., Chem. Soc. Rev. **38**, 2532 (2009)
2. G. Reiss, A. Hutten, Nat Mater **4**, 725 (2005)
3. C. Wang, H. Daimon, S.H. Sun, Nano Letters **9**, 1493 (2009)
4. B.V. Harbuzaru, A. Corma, F. Rey et al., Angewandte Chemie-Int. Edn. **47**, 1080 (2008)
5. J. Hassoun, S. Panero, P. Simon et al., Adv. Mater. **19**, 1632 (2007)
6. R.M. Wang, O. Dmitrieva, M. Farle et al., Phys. Rev. Lett. **100**, 017205 (2008)
7. Y.H. Wang, W. Wei, D. Maspoch et al., Nano. Lett. **8**, 3761 (2008)
8. H.B.R. Lee, G.H. Gu, J.Y. Son et al., Small **4**, 2247 (2008)
9. N. Wang, L. Guo, L. He et al., Small **3**, 606 (2007)
10. L. Sandoval, H.M. Urbassek, Nano. Lett. **9**, 2290 (2009)
11. G.D. Mahan, Phys. Rev. Lett. **102**, 016801 (2009)
12. W. Zhou, K. Zheng, L. He et al., Nano. Lett. **8**, 1147 (2008)
13. N. Du, H. Zhang, B. Chen et al., Adv. Mater. **19**, 4505 (2007)
14. H.L. Hu, K. Sugawara, Chem. Phys. Lett. **477**, 184 (2009)
15. B.P. Jia, L. Gao, J. Phys. Chem. C Nanomater. Interfaces **112**, 666 (2008)
16. J.G. Zhang, J. Chen, Z.X. Wang, Mater. Lett. **61**, 1629 (2007)
17. Z.B. He, Y. Shu-Hong, X.Y. Zhou et al., Adv. Funct. Mater. **16**, 1105 (2006)
18. H.L. Niu, Q.W. Chen, M. Ning et al., J. Phys. Chem. B **108**, 3996 (2004)
19. J.H. Wang, Y.W. Ma, K. Watanabe, Chem. Mater. **20**, 20 (2008)
20. X. Zhang, W.M. Liu, Mater. Res. Bull. **43**, 2100 (2008)
21. X.J. Yu, O. Wilhelmi, H.O. Moser et al., J. Electron. Spectros. Relat. Phenomena. **144**, 1031 (2005)
22. L.F. Mattheiss, R.E. Dietz, Phys. Rev. B **22**, 1663 (1980)
23. J.H. Gao, B. Zhang, X.X. Zhang et al., Angewandte Chemie-Int. Edn. **45**, 1220 (2006)
24. Z.W. Liu, P.C. Chang, C.C. Chang et al., Adv. Funct. Mater. **18**, 1573 (2008)
25. R. Yanes, O. Chubykalo-Fesenko, H. Kachkachi et al., Phys. Rev. B **76**, 064416 (2007)
26. R. Skomski, J. Phys. Condens. Matter. **15**, R841 (2003)
27. L. He, W.Z. Zheng, W. Zhou et al., J. Phys. Condens. Matter. **19**, 036216 (2007)
28. P.M. Paulus, F. Luis, M. Kroll et al., J. Magn. Magn. Mater. **224**, 180 (2001)
29. V. Bliznyuk, S. Singamaneni, S. Sahoo et al., Nanotechnology **20**, 105606 (2009)